Novel Modeling and Damping Technique for Hybrid Stepper Motor

Kenneth W. H. Tsui,
ASM Assembly Automation Ltd.,
4/F Watson Centre, 16 Kung Yip Street,
Kwai Chung, Hong Kong

Norbert C. Cheung,
Department of Electrical Engineering,
The Hong Kong Polytechnic University,
Hunghom, Kowloon, Hong Kong

***Abstract*– It is well known that commercial hybrid stepper system has one or more low speed resonant points. However, this characteristic is not accurately modeled without high order equations or complicated measurement of motor parameters. In this paper, a novel approach is proposed to model the behavior of a commercial 1.8° hybrid stepper motor accurately and efficiently. Damping algorithms for open loop and servo control are proposed. Both simulation and experiment results show that the proposed algorithms can effectively eliminate low speed resonance and vibration of the stepper system.**

I. INTRODUCTION

Stepper motor system has several significant advantages. No feedback is normally required for either position control or speed control. Positional error is non accumulative. Besides, stepper motors are compatible with modern digital equipment. For these reasons, various types and classes of stepping motor have been used in computer peripheral, automated machinery and similar system [1]. Cost of stepper system is significantly lower than that of servo system. It is mainly because of removal of high cost of position feedback device and complicated feedback control. Moreover, it does not require tuning of feedback control which needs extra expertise and effort. Simple hardware and control configuration also improve system reliability.

One of the most unfavorable features of stepper motor is mechanical resonance, especially at low speed (say, below 300rpm). The problem is less significant at high speed because the vibration exceeds the bandwidth of most mechanical system. Resonance prevents stepper motor to run steadily at certain speed and reduce usable torque. Also, this prevent stepper motor to be used on application than require smooth low speed motion.

The frequency of oscillation can be predicted for any motor/ load combination from the static torque/ rotor position characteristic, provided the system is lightly damped. The natural frequency of rotor oscillation about the equilibrium position is [2]

$$f_n = \frac{1}{2\pi}\sqrt{\frac{T'}{J}} \tag{1}$$

T': stiffness of the τ/θ characteristic. J : Rotor inertia, kg m^2. f_n : Natural frequency, Hz.

Possible excitation of the vibration includes discrete stepping motion, detent torque of permanent magnet, pole to pole variation, etc. With the popularity of micro-step drive, stepping ripple had been greatly minimized. However, even if we use very fine micro-stepping, vibration and resonance still exist due to motor characteristics.

Effort has been spent on improving the performance of stepper system in various ways. Zribi and Chiasson implemented the position control by exact feedback linearization [4]. Chen et al. improved profile tracking performance by model based feedback controller with a least-squares based identification procedure [5]. Goodnick reported satisfactory result of electronic damping based on a torque observer [6]. Yang and Kuo reported effective damping algorithm based on a PLL position and velocity observer [7]. However, some of the mentioned algorithms are feedback based which require complicated parameter identification and high resolution position feedback. The others which are sensorless based, requires large amount of computation. Therefore, they may not be cost effective enough to be implemented on a commercial system. The need of effective and efficient damping algorithm still exists.

Simplified stepper model is used most of the time for efficiency. The simplified stepper electrical dynamics and torque expression are shown here [3].

$$\frac{di_a}{dt} = -\frac{R}{L_o} i_a + \frac{K_m}{L_o}\omega \sin(N_r\theta) + \frac{v_a}{L_o} \tag{2}$$

$$\frac{di_b}{dt} = -\frac{R}{L_o} i_b - \frac{K_m}{L_o}\omega \sin(N_r\theta) + \frac{v_b}{L_o} \tag{3}$$

$$\tau = K_m\left[-i_a \sin(N_r\theta) + i_b \cos(N_r\theta)\right] - K_{d4}\sin(4N_r\theta) \tag{4}$$

τ : Torque output (Nm). K_m : Force constant (Nm/ A). N_r : Number of pole pair. θ : Rotor position (rad). K_{d4} : Amplitude of 4th harmonic detent torque (Nm).

With micro-stepping control, the simplified model predicts only one resonant speed, which is caused by detent torque, the last term in (4). However, this does not match with that of a commercial stepper in real life. For example, the studied motor has three resonant speeds, which will be shown in later investigation. In this paper, new stepper torque expression is proposed to model this characteristic without using high order equations and complicated identification procedures. Model based damping algorithms are proposed for both open loop and servo mode. Both simulation and experimental results

show that the proposed algorithms can effectively eliminate the resonance and vibration at low speed.

II. MODELING OF STEPPER MOTOR

A. System for Investigation

The block diagram of the hardware platform for our investigation is shown in Figure 1. The controller is based on TI 2810 DSP which performs motion control, profile generation and current control. The controller is programmed and commanded by a standard PC through JTAG interface. It outputs PWM signals at 20 kHz to control a chopper power drive which outputs are connected to our investigated motor. Isolated current sensing is used to provide current feedback to the controller. A commercial 1.8º hybrid stepping motor is chosen for our studies. It is a Sanyo Denki 103H7126-0722, with coil resistance 0.9Ω, coil inductance 2.2mH, rotor inertia $0.36\times10^{-4} kg\cdot m^2$, rated current 3A and torque 1.27 Nm. An optical encoder (1000 line, 4000 pulse/rev) is attached to the motor for performance monitoring and position control in servo mode.

B. Proposed Stepper Model

The system mentioned above is configured to open loop control, holding current is set at 1.9A. The natural frequency of the system calculated by (1) is 142Hz. On driving the motor with smooth sinusoidal current, 3 resonant speeds are observed at about 43, 86 and 173 rpm. These correspond to driving current at 36, 72 and 144 Hz. They are likely to be caused by detent torque. At the 1st resonance (43rpm/ 36Hz), by using (4), it is easy to observe that the frequency of detent torque ripple is $36Hz\times4=144Hz$, which matches with the calculated system natural frequency (142Hz). Therefore, the 1st resonance is excited by 4th harmonic detent torque ripple. For the 2nd and 3rd resonance, they occur at doubled speed of previous resonance. Thus, there should be 2nd and 1st harmonic detent torque component which excite the resonances. A torque expression (5) to describe this characteristic is proposed. Note that dynamic friction is assumed zero for low speed operation.

$$\tau = K_m\left[-i_a\sin(N_r\theta)+i_b\cos(N_r\theta)\right]-K_{d4}\sin(4N_r\theta) - K_{d2}\sin(2N_r\theta+\phi_2)-K_{d1}\sin(N_r\theta+\phi_1)-F_s \quad (5)$$

K_{d1}: Amplitude of 1st harmonic torque ripple (Nm). ϕ_1: Phase shift of 1st harmonic torque ripple (rad). K_{d2}: Amplitude of 2nd harmonic torque ripple (Nm). ϕ_2: Phase shift of 2nd harmonic torque ripple (rad). F_s: Static friction (Nm).

C. Motor Characteristic Identification

To fill in the constants K_{d4} K_{d2} K_{d1} ϕ_2 ϕ_1 F_s in (5), we need to identify the characteristic of the studied stepper motor. The stepper system described in part A. is set to run in servo mode with the control algorithm described in (6) and (7). Block diagram of the model of servo system is shown in Figure 2 for reference. K_m is set to 0.3 and N_r is set to 50 as given by motor specification. θ_{fb} is obtained from optical encoder feedback.

$$i_{d\_cmd}=0 \quad (6)$$

$$i_{q\_cmd}=\frac{1}{K_m}\left[\begin{array}{r}K_{d4}\sin(4N_r\theta_{fb})+K_{d2}\sin(2N_r\theta_{fb}+\phi_2)\\+K_{d1}\sin(N_r\theta_{fb}+\phi_1)+F_s\end{array}\right] \quad (7)$$

Current control is done by digital PI current loop. K_p and K_i are proportional gain and integration gain of the current loop respectively.

$$v_d=K_p\left(i_{d\_cmd}-i_{d\_fb}\right)+K_i\int\left(i_{d\_cmd}-i_{d\_fb}\right)dt \quad (8)$$

$$v_q=K_p\left(i_{q\_cmd}-i_{q\_fb}\right)+K_i\int\left(i_{q\_cmd}-i_{q\_fb}\right)dt \quad (9)$$

Motor phase current i_a i_b are transformed to i_d i_q by the well known Park or Direct- Quadrature (DQ) transformation [3].

$$\begin{bmatrix}i_d\\i_q\end{bmatrix}=\begin{bmatrix}\cos(N_r\theta_{fb}) & \sin(N_r\theta_{fb})\\-\sin(N_r\theta_{fb}) & \cos(N_r\theta_{fb})\end{bmatrix}\begin{bmatrix}i_a\\i_b\end{bmatrix} \quad (10)$$

External torque is applied to turn the shaft of the motor. The constants to be found are tuned until minimum resistive torque is observed and periodic torque ripple is removed. The results of the identification are $K_{d4}=0.006$, $K_{d2}=0.014$, $K_{d1}=0.011$, $\phi_2=\pi$, $\phi_1=\pi/2$, $F_s=0.029$ (clockwise), $F_s=-0.029$ (anit-clockwise).

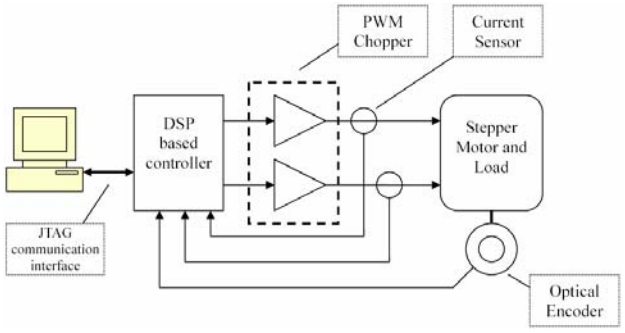

Figure 1 Block diagram of the stepper system for investigation.

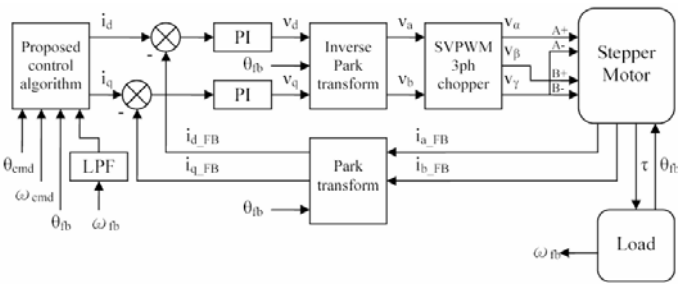

Figure 2 Block diagram of the model of servo stepper system.

III. OPEN LOOP DAMPING ALGORITHM

A. *The Damping Algorithm*

Based on the proposed torque expression (5) and the identified motor characteristic, the MatLab model of an open loop system is build as illustrated in Figure 3. Control algorithm (11) (12) is proposed to damp out the resonances. The three terms of i_{q_cmd} (12) are 4th, 2nd and 1st harmonic torque compensation. Constants obtained in section II. C. will be substituted into (12).

$$i_{d\_cmd} = 1.9 \tag{11}$$

$$i_{q\_cmd} = \frac{1}{K_m}\left[\begin{array}{l} K_{d4}\sin(4N_r\theta_{cmd}) + K_{d2}\sin(2N_r\theta_{cmd}+\phi_2) \\ \qquad + K_{d1}\sin(N_r\theta_{cmd}+\phi_1) \end{array}\right] \tag{12}$$

PI current control is described by (8) (9) in previous section. For Park Transformation, it is basically the same as (10) with θ_{fb} replaced by position command θ_{cmd}. Assume rigid mounting of dummy load without load torque. The load is described by (13). D is damping factor which is assumed to be 0.001 $Nm/rad\ s^{-1}$ for a lightly damped system.

$$\begin{bmatrix}\dot{\theta}\\ \dot{\omega}\end{bmatrix} = \begin{bmatrix}0 & 1\\ 0 & 0\end{bmatrix}\begin{bmatrix}\theta\\ \omega\end{bmatrix} + \begin{bmatrix}0\\ 1\end{bmatrix}\left[-\frac{D\omega}{J} + \frac{\tau}{J}\right] \tag{13}$$

With reference to the works of Yang et al. [8], the three phase SVPWM driving scheme is described by (14) – (17).

$$\begin{bmatrix}v_\alpha\\ v_\beta\\ v_\gamma\end{bmatrix} = \begin{bmatrix}1 & 0 & 1\\ 0 & 1 & 1\\ 0 & 0 & 1\end{bmatrix}\begin{bmatrix}v_a\\ v_b\\ v_o\end{bmatrix} \tag{14}$$

$$v_{\max} = Maximum\left\{v_a, v_b, 0\right\} \tag{15}$$

$$v_{\min} = Minimum\left\{v_a, v_b, 0\right\} \tag{16}$$

$$v_o = \frac{v_i}{2} - \frac{\left(v_{\max} + v_{\min}\right)}{2} \tag{17}$$

In addition, zero-order hold is applied on $v_\alpha\ v_\beta\ v_\gamma$ to simulate the periodic PWM update of chopper drive.

B. *Simulation Results*

In all simulations, the command is a speed ramp from 0 rpm at t = 0 to 200 rpm at t = 0.8 s. In the first case (Figure 8), no damping is applied, therefore $i_{q\_cmd} = 0$. Three resonant speeds are observed at about 45, 80 and 170 rpm which match with the 43, 86 and 173 rpm observed in experiment. With the injection of 4th harmonic torque compensation, the 1st resonance is damped out (Figure 5, an arrow is put to mark the 1st resonance). Similarly, injection of 2nd and 1st harmonic torque compensation can damp out the 2nd and 3rd resonances respectively (Figure 6 and Figure 6). Amplitude of velocity error is most significant at 2nd resonance which is caused by the relatively large 2nd harmonic detent torque ripple. Figure 8 shows the results of injection of all the three harmonic torque compensation in i_{q_cmd}. The velocity ripple is almost completely eliminated in the whole low speed range.

Note that at all three resonances, frequency of the velocity error is the same which corresponds to the natural frequency f_n of the system (calculated to be 144 Hz). Besides, if load torque is applied, the damping performance is expected to degrade. It is because the equilibrium position of the rotor will shift a certain degree from the original position. Fine tuning of ϕ_1 and ϕ_2 will be needed to offset the change.

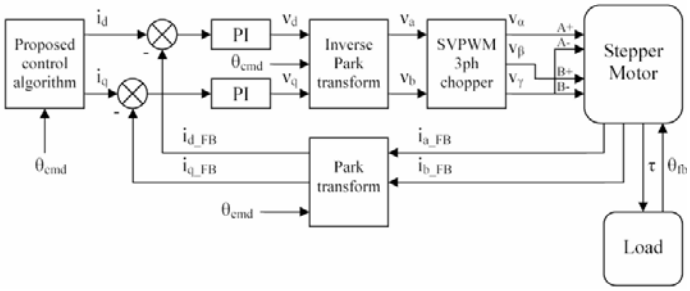

Figure 3 Block diagram of the model of open loop stepper system.

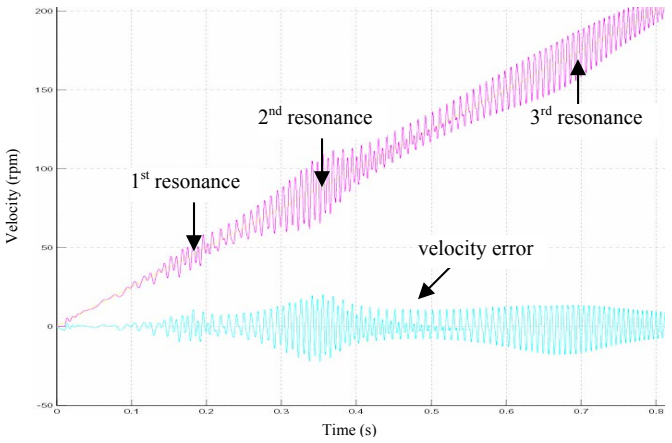

Figure 4 Simulated velocity feedback (red) and error (blue) of open loop system without damping.

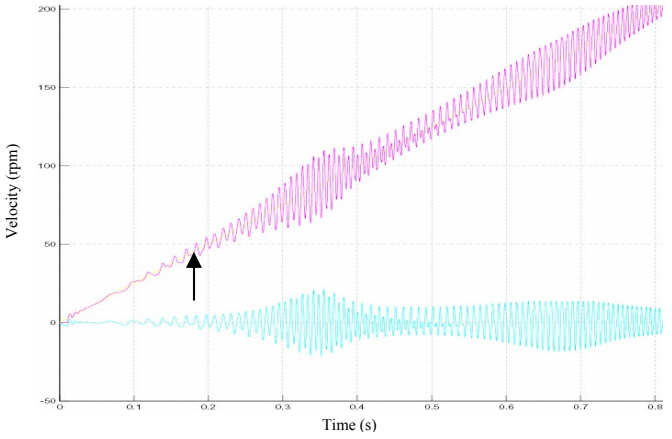

Figure 5 Removal of 1st resonance by injection of 4th harmonic torque compensation.

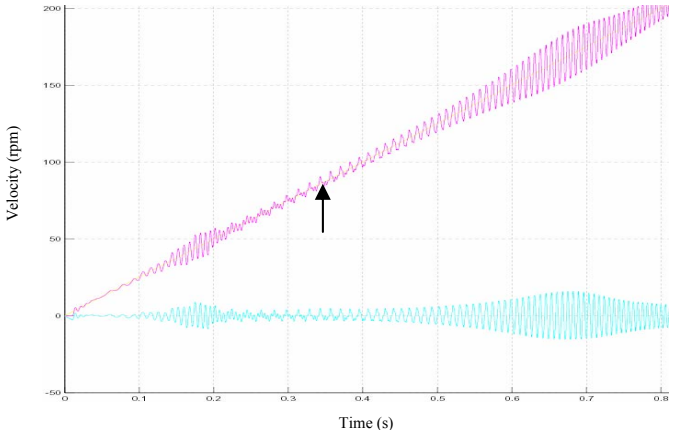

Figure 6 Removal of 2nd resonance by injection of 2nd harmonic torque compensation.

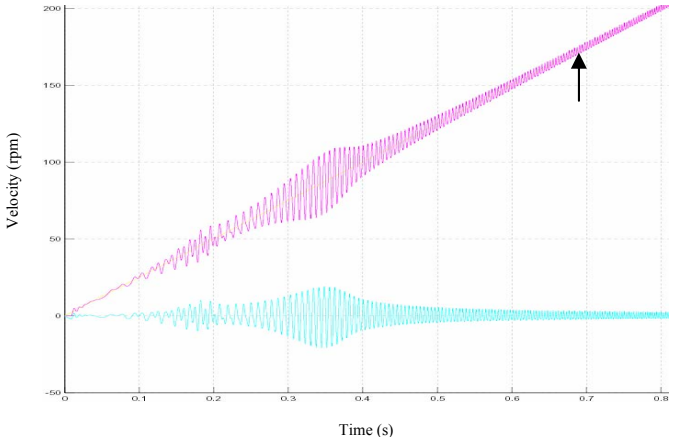

Figure 7 Removal of 3rd resonance by injection of 1st harmonic torque compensation.

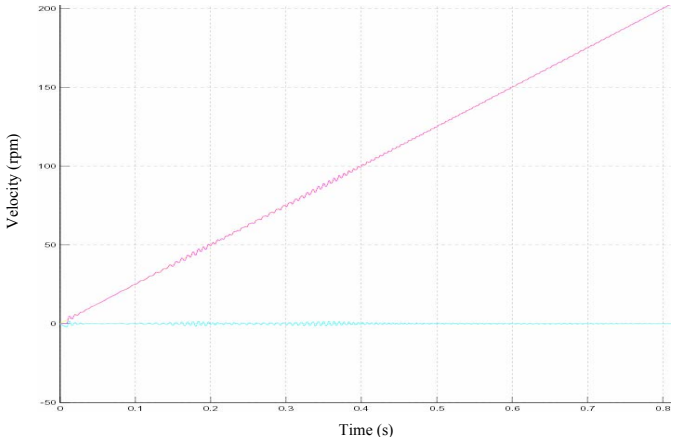

Figure 8 Removal of all three resonances by injection of 1st 2nd and 4th harmonic torque compensation.

C. *Experiment Results*

The motor is set to run at constant velocity at the 1st (43rpm), 2nd (86rpm) and 3rd (173rpm) resonant velocity to observe the effect of the proposed damping algorithm. The 1st resonance is damped out by the injection of 4th harmonic torque compensation (**Figure 9**). The 2nd resonance is damped out by injection of 2nd harmonic torque compensation (Figure 10). The 3rd resonance is damped out by injection of 1st harmonic torque compensation (Figure 11). Note that the frequency of velocity error is the same in all three resonances. This means that they are caused by the same mechanical natural frequency. However, they are triggered by torque ripple of three different harmonics. Resonance occur when the frequency of any one of the torque ripple harmonics match with the natural frequency. The experimental results match well with those of simulation. Note that the high frequency ripple is the differentiation noise of QEP based velocity measurement.

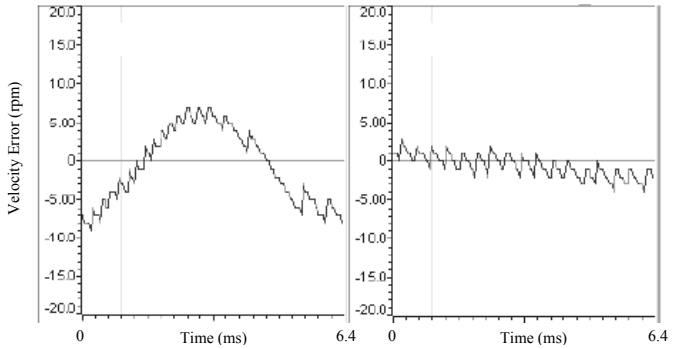

Figure 9 Experimental results of velocity error at 43 rpm, without damping (left) and with damping (right).

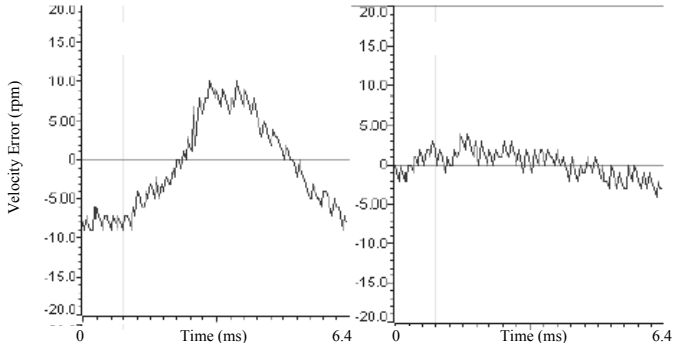

Figure 10 Velocity error at 86 rpm, without damping (left) and with damping (right).

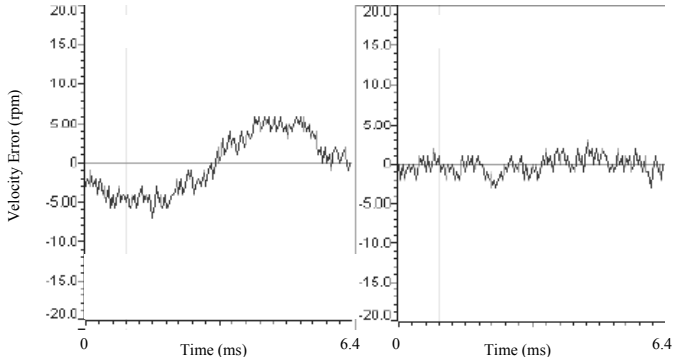

Figure 11 Velocity error at 173 rpm, without damping (left) and with damping (right).

IV. SERVO MODE DAMPING ALGORITHM

A. The Damping Algorithm

MatLab model of a servo controlled stepper system is built as illustrated in Figure 2. Damping algorithm (18) (19) is proposed for smooth low speed servo motion. The first three terms of (19) are for position control where K_{p_vel}, K_{p_pos} and K_{i_pos} are control parameters of the standard position PID loop. The four terms afterward are torque ripple compensation at 4th, 2nd, 1st harmonics and static friction compensation.

$$i_{d\_cmd} = 0 \tag{18}$$

$$i_{q\_cmd} = \frac{1}{K_m}\begin{bmatrix} K_{p\_vel}\omega_{err} + K_{p\_pos}\theta_{err} + K_{i\_pos}\int \theta_{err}\, dt \\ + K_{d4}\sin(4N_r\theta_{fb}) + K_{d2}\sin(2N_r\theta_{fb} + \phi_2) \\ + K_{d1}\sin(N_r\theta_{fb} + \phi_1) + F_s \end{bmatrix} \tag{19}$$

where $\omega_{err} = \omega_{cmd} - \omega_{fb}$ and $\theta_{err} = \theta_{cmd} - \theta_{fb}$

B. Simulation Results

Simulated velocity feedback and error of the system are shown in Figure 12 and Figure 13. In both simulations, the command is a speed ramp from 0 rpm at t = 0 to 100 rpm at t = 1 s. In the first case (Figure 12), no damping is applied, only position PID controller. The smoothness of the motions is unsatisfactory. Figure 13 shows the results with injection of torque compensation components in i_{q_cmd} as described in (19). The smoothness of the motion is significantly improved. Note that some high frequency ripple is observed before t = 0.1s. This is caused by the quantization noise of encoder position feedback which results in noise in the position loop. The effect of finite resolution of encoder is modeled by quantization of θ_{fb}. For our investigated system, the encoder is 4k pulse/rev. This means the position resolution is only 20 counts per step with our 200 step/rev stepper motor. It is expected to limit system position and current control accuracy.

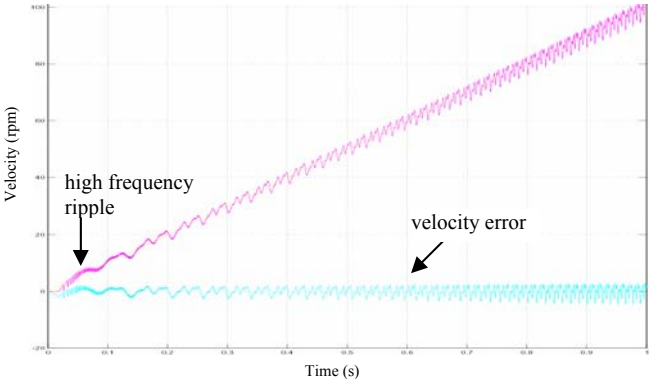

Figure 12 Simulated velocity feedback (red) and error (blue) of servo system without damping.

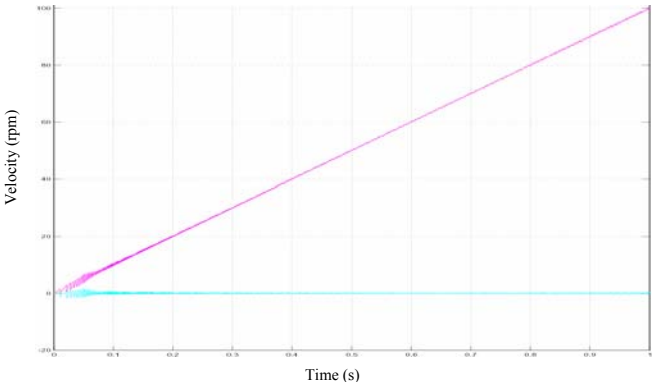

Figure 13 Simulated velocity feedback (red) and error (blue) of servo system with proposed damping algorithm.

C. Experiment Results

Experiment is done to verify the simulation results. The system is set to move at low speed without damping. Therefore, K_{d1} K_{d2} K_{d3} and F_s of (19) are set to 0. Significant vibration is observed at any speed under 100rpm. Then, proposed damping algorithm is applied and smooth motion down to 30rpm is observed.

As velocity feedback is found by differentiating position feedback, the resolution of the velocity depends on the sample rate as well as the resolution of the encoder [9]. In our system for investigation, encoder resolution is 4k pulses/ rev and the calculation is done at 20 kHz. This means the resolution is $1/4000 \times 20k \times 60 = 300$rpm! A low pass filter is needed to filter the velocity feedback. However, the LPF makes the system less responsive to correct velocity error. LPF in the experimental system is implemented by a first order digital IIR at 32Hz bandwidth.

V. CONCLUSION

The characteristic of a commercial stepper motor is successfully modeled by the proposed torque expression. Simulation and experimental results show that the proposed damping algorithm can effectively eliminate low speed resonance and vibration in both open loop and servo mode. More works will follow to study its application issue and parameter sensitivity.

ACKNOWLEDGMENT

The authors gratefully acknowledge the contributions of Mr. S. W. Tam and Dr. W. C. Gan for their helpful suggestions. The authors wish to thank ASM Assembly Automation and the Hong Kong Polytechnic University for the support of this project through the Teaching Company Scheme (project code: ZW82)

REFERENCES

[1] Takashi Kanjo, and Akira Sugawara, "Stepping Motors and Their Microprocessor Controls" *Clarendon Press,* Oxford, 1994.

[2] Paul Acarnley, "Stepping Motors a guide to theory and practice", 4th

ed., *The Institution of Electrical Engineers,* Stevenage, UK, 2002.

[3] F. Khorrami, P. Krishnamurthy, and H. Melkote, "Modeling and Adaptive Nonlinear Control of Electric Motors", *Springer – Verlag Berlin Heidelberg New York,* 2003

[4] M. Zribi and J. Chiasson, "Position Control of a PM Stepper Motor by Exact Linearization", *IEEE Transactions on Automatic Control,* Vol. 36, No. 5, pp.620 – 625, May 1991

[5] W.D. Chen, K.L. Yung, and K.W. Cheng, "Profile Tracking Performance of a Low Ripple Hybrid Stepping Motor Servo Drive", *IEE Proc.–Control Theory Appl.,* Vol. 150, No. 1, pp.69 – 76, January 2003

[6] Stuart Goodnick, "Electronic Damping Cures Step Motor Resonance – Part II: Damping Technique", *Power Conv. Intell. Motion,* pp.32-43, May 1997.

[7] Sheng-Ming Yang and Ei-Lang Kuo, "Damping a Hybrid Stepping Motor with Estimated Position and Velocity", *IEEE Transactions on Power Electronics,* Vol. 18, No. 3, pp.880 – 887, May 2003.

[8] Sheng-Ming Yang, Feng-Chieh Lin, and Ming-Tsung Chen, "Micro-Stepping Control of a Two-Phase Linear Stepping Motor With Three-Phase VSI Inverter for High-Speed Applications", *IEEE Transactions on Industry Applications*, Vol. 40, No.5, pp.1257 – 1264, Sep/ Oct 2004.

[9] Marc Bodson, John N. Chiasson, Robert T. Novotnak, and Ronald B. Rekowski, "High-Performance Nonlinear Feedback Control of a Permanent Magnet Stepper Motor", *IEEE Transactions on Control Systems Technology,* Vol.1, No. 1, pp.5 – 14, March 1993.